



**HAL**  
open science

## **SD electronics: simulations on the dynamic range**

I. Lhenry-Yvon, T. Suomijarvi, B. Genolini, T. Nguyen Trung, E. Parizot, J. Pouthas

► **To cite this version:**

I. Lhenry-Yvon, T. Suomijarvi, B. Genolini, T. Nguyen Trung, E. Parizot, et al.. SD electronics: simulations on the dynamic range. 2001, pp.11. in2p3-00010529

**HAL Id: in2p3-00010529**

**<https://hal.in2p3.fr/in2p3-00010529>**

Submitted on 24 Oct 2001

**HAL** is a multi-disciplinary open access archive for the deposit and dissemination of scientific research documents, whether they are published or not. The documents may come from teaching and research institutions in France or abroad, or from public or private research centers.

L'archive ouverte pluridisciplinaire **HAL**, est destinée au dépôt et à la diffusion de documents scientifiques de niveau recherche, publiés ou non, émanant des établissements d'enseignement et de recherche français ou étrangers, des laboratoires publics ou privés.

**IPNO DR-01-009**

**SD electronics: simulations on the dynamic range**

Lhenry-Yvon, T. Suomijärvi, B. Genolini,  
T. Nguyen Trung, E. Parizot, J. Pouthas

*Institut de Physique Nucléaire d'Orsay,  
91406 Orsay cedex, France*

## **SD electronics: simulations on the dynamic range**

**I. Lhenry-Yvon, T. Suomijärvi, B. Genolini, T. Nguyen Trung, E. Parizot, J. Pouthas,  
Institut de Physique Nucléaire,  
IN2P3/CNRS,  
91406 Orsay, Cedex, France**

### **Abstract**

The surface detector electronics of the Pierre Auger Observatory is characterized by a large dynamic range due to the variation of the signal intensity of the Cherenkov tanks as a function of the distance from the core. In this paper, we present results of simulations and discuss the impact of the dynamic range on the shower reconstruction.

### **Introduction**

The Pierre Auger Observatory (PAO) surface array consists of cylindrical Cherenkov water tanks having a height of 1.2 m and a 10 m<sup>2</sup> cross section [1]. The tanks are lined with UV reflecting PE-Tyvek lamination bags and filled with high purity water. When impinging the water tanks, shower particles (muons, electrons and gammas) emit Cherenkov radiation. The light produced in the tank is detected by three large photomultipliers (PMT) viewing the tank from the top. Each PMT has two output signals [2,3], one from the anode and the other from the last dynode. The dynode signal is amplified and is used to measure with high precision the lower part of the dynamic range (typically up to about 1000 photoelectrons) while the anode signal is used to measure over the total dynamic range. Both signals are digitalized by using “flash” converters (FADC) having a sampling rate of 40 MHz and a memory of 10 bits[4].

The amount of light produced in the Cherenkov tank varies from a few photoelectrons for tanks far away from the shower core to more than 100 000 photoelectrons (PEs) for tanks close to the core. From the experimental point of view the upper limit of the dynamic range must be large enough to allow us to reconstruct the energy of the primary particle, which is inferred from the signal density. Concerning Haverah Park data [5], the energy was estimated using the signal density per square meter in water tanks at the distance of 600 m from the shower core ( $\rho(600)$ ). Due to the larger spacing between the tanks in the case of the PAO array the energy will be determined from the signal density at 1000 m [1]. As discussed in ref. [6], at a distance of 1000 m, one observes only slight deviations from the standard relation between energy and signal density and modest dependence on the primary composition. In order to have an accurate interpolation of the lateral profile around this value (1000 m), it is crucial to have non-saturated signals from tanks below 1000 m. These considerations together with the requirement for a good precision in the geometrical reconstruction will tend to increase the upper limit of the dynamic range.

The lower limit of the dynamic range is determined by the characteristics of the signals issued from tanks far away from the shower core. These signals are weak and spread over a long time period, yielding typically peak values of a few PEs. They are important for the discrimination of electromagnetic and muonic components of the shower. Furthermore, the calibration of the tanks and

electronic response will be performed through the analysis of the random muons from low energy cosmic rays, which will also require accurate measurement at the level of a few PEs.

In this paper, we will discuss the impact of the dynamic range on the shower reconstruction and on the calibration. Simulations of the detection of some typical showers as well as background muons will be presented. The characteristics of the simulations will be described in the first section. The second section discusses the lower limit of the dynamic range and the calibration and the third one is devoted to the upper limit.

## Simulations

The atmospheric shower simulations were performed with the simulation package AIRES [7] using the QGSJET [8] interaction model. Different primary particles (protons, irons and gammas) were considered with energies ranging from  $2 \cdot 10^{19}$  eV to  $10^{21}$  eV and with incident angles of  $0^\circ$  (vertical shower) and  $30^\circ$ . The thinning parameter used in the AIRES simulation was set to  $10^{-7}$ . The sampling of the ground particles and the simulation of the tank response were performed with the detector simulation code of Pierre Billoir [9] which samples the ground particles in the tank array and then simulates the Cherenkov radiation and light collection in the tank. The muons are assumed to go through the tank and to produce a uniform radiation rate along their path while photons and electrons are assumed to stop in the tank and lose their energy on the basis of 200 MeV per meter. The radiated energy is eventually converted into photoelectrons detected at the photocathode of each photomultiplier according to a maximal photocathode efficiency of 25%. The time attributed to each PE corresponds to the arrival time of the incoming particle randomized over 150 ns in order to take into account the tank response.

Figure 1a displays the time distributions resulting from a simulation for a vertical 500 EeV proton shower and figure 1b shows the same distributions for a  $20^\circ$  100 EeV proton shower. The time profile of the PEs collected at the photocathode varies rapidly as a function of the distance from the shower core. Near the shower core the spectrum is dominated by a large electromagnetic peak located below 500 ns. At larger distances the signal is strongly attenuated, the time spread becomes larger and the proportion of muon-induced photoelectrons relative to the total signal increases. In this case, the dynamic range extends from a few PEs/ns at large distances to about 1000 PEs/ns at 500 m from the core. Furthermore, it can be seen that in order to measure properly the lateral shower profile, a large time window (above 10  $\mu$ s) is needed.

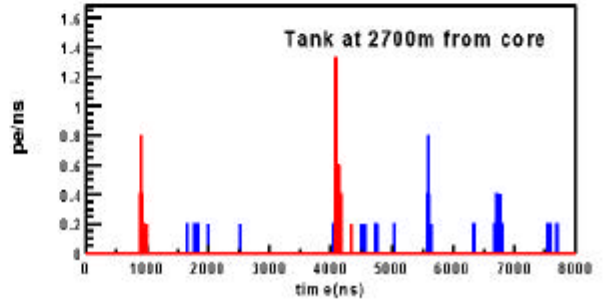
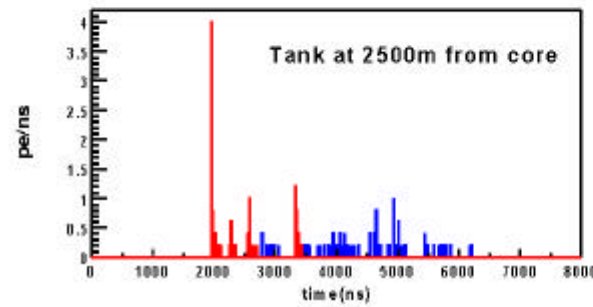
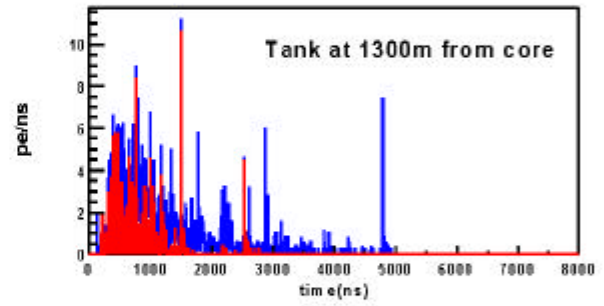
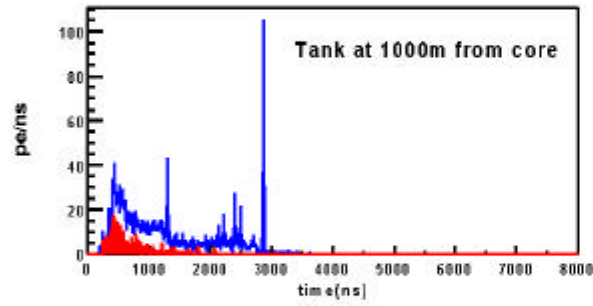
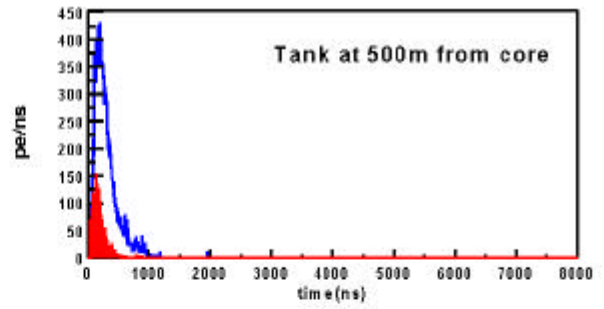
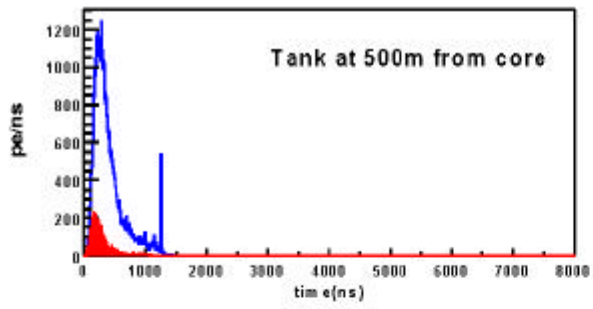


**Figure 1-a.** Distribution of photoelectrons for one PMT as a function of time for a 500 EeV vertical proton shower detected in tanks at 500, 1000 and 2500 m from the shower core. The blue line corresponds to the total distribution and the red filled spectrum shows the muon contribution.

**Figure 1-b.** Same as Figure 1-a for a 100 EeV  $20^\circ$  proton shower detected in tanks at 500, 1300 and 2600 m.

### The calibration and the lower limit on the dynamic range.

As recalled in the introduction, it is crucial that the dynamic range allows a reliable calibration of the ADC traces. An ideal absolute calibration of the PMTs would be based on a single photoelectron spectrum. However, this will be very difficult in our experimental conditions since the PMTs are operated with a relatively low gain ( $2 \cdot 10^5$ ) and the sampling rate of the FADC is only 40 MHz.

An appealing possibility is to use the background muons for calibration as already discussed in several GAP-notes [10-13,15]. The total flux of charged particles at the ground level is about  $180 \text{ s}^{-1} \text{ m}^{-2}$ , 75% of this being penetrating muons and the rest soft muons and electrons [14]. The energy distribution of muons ranges from  $10^1$  to  $10^2$  GeV, with a maximum at 1 GeV, and the angular distribution follows a  $\cos^2\theta$  law. We have simulated background muons spectra by using the previously described fast detector simulation code. The charge spectrum was calculated for 10000 simulated vertical muons hitting the middle of the Cherenkov tank and for 10000 random muons whose angle followed the  $\cos^2\theta$  angular distribution. Only a fixed energy of 1 GeV was considered in these simulations. The results are displayed in Figure 2. It is observed that the mean number of photoelectrons at the photocathode measured by one PMT is about 30 for both vertical and random muons but the distribution of random muons is much larger than the distribution of vertical ones.

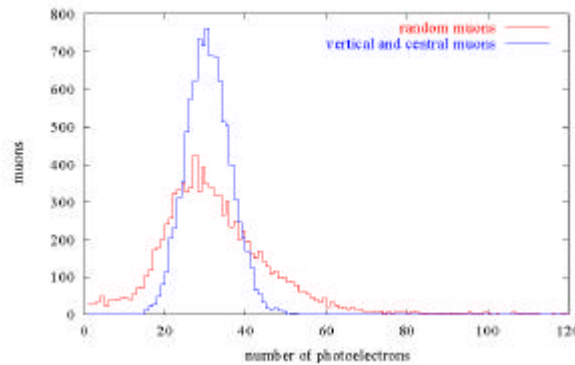


**Figure 2.** Simulated spectrum for vertical muons and random muons.

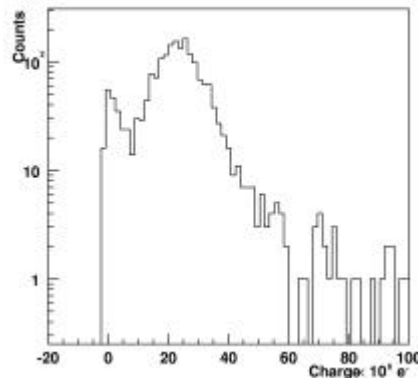


**Figure 3.** Charge spectrum measured from telescope triggered muons. Absorbing material was put between the scintillators to eliminate the soft electromagnetic background. An oscilloscope with a sampling of 1GHz was used for the data acquisition. In this setup, one VEM corresponds to  $2.3 \cdot 10^7 e$ .

These results are in agreement with the measurements presented in ref. [12] and [13] and with the more recent measurements performed at the Galpon test tank [15]. Figure 3 shows a muon telescope triggered spectrum. The data was analyzed requiring coincidence between 2 PMTs. It can be seen that even though some electromagnetic background is remaining in the lower part of the spectrum, a clear maximum can still be seen, at a value very close to that from the simulation. It should be noted that a more complete analysis of the data is in progress [16].

These measurements give confidence in the simulated muon response of the tanks. They show that the average number of photoelectrons induced by a vertical muon is close to 30 (integrated in about 150 ns). In the simulation, the maximum number of photoelectrons per 25ns is about 8. The proper determination of the integrated number of photoelectrons per muon requires a reliable measurement of signals at the level of a few photoelectrons. Considering the digitization of the signal, the low part of the dynamic range cannot be compressed to more than a photoelectron per ADC channel.

### Upper limit of the dynamic range

The PMTs are required to work linearly for output currents up to 50 mA. The amplifiers used for the dynode signal, with a 50  $\Omega$  load, saturate at 2V, leading to an upper limit for the dynode current of 40 mA. The resulting signals are conditioned to match the input ADC range. The total dynamic range is coded by two 10 bits ADCs. The first ADC is used to code the high gain channel (amplified dynode signal) and will be calibrated with the method described in the previous section. The second ADC codes the low gain channel (anode signal) and has to be cross calibrated with the high gain channel. A sufficiently large overlap between the two channels is thus necessary. The dynode amplification factor is 32 ( $2^5$ ), yielding a total dynamic range of  $2^{15}=3.3 \cdot 10^4/25\text{ns}$ .

The nominal operating gain of the PMT was chosen to be  $2 \cdot 10^5$ . It will be adjusted depending on the maximum current considered at the photocathode, in order to cover its output linear range up to 40 mA. Table 1 shows the influence of the gain value on the limits of the dynamic range and on the FADC calibration.

Gain value	Maximum signal	Photocathode current	Low gain FADC calibration	High gain FADC calibration
$1.6 \cdot 10^5$	$4 \cdot 10^4$ PE/25ns	250nA	39 PE/channel	1.2 PE/channel
$2 \cdot 10^5$	$3.2 \cdot 10^4$ PE/25ns	200nA	31 PE/channel	0.96 PE/channel
$3 \cdot 10^5$	$2 \cdot 10^4$ PE/25ns	128nA	20 PE/channel	0.6 PE/channel

**Table 1.** Calibration of the FADC as a function of the gain value. The maximum signal corresponds to a 40 mA output current at the anode.

The table shows that in order to respect the lower limit on the dynamic range given above (less than 1 PE/Channel), it won't be possible to measure photocathode current up to 200 nA. A cutoff value will be imposed to the upper limit of the dynamic range.

In the following, we will try to study, with the help of simulations, the effect of different cutoff values on the shower reconstruction. As discussed in the introduction, the upper limit to be set on the dynamic range depends on the closest distance at which shower particles should be detected. It was required that 1 ZeV shower particles could be detected at 500 m from core [2]. A simulation for this case is shown in Figure 4a. The maximum number of PEs/ns in a tank at 500 m is of the order of 2000 for each PMT, or  $5 \cdot 10^4$  PEs/25ns. Figure 4-b shows the corresponding time distribution of photoelectrons at the photocathode. The corresponding photocathode current is about 300 nA, which is higher than the current that can be measured in the operating mode.

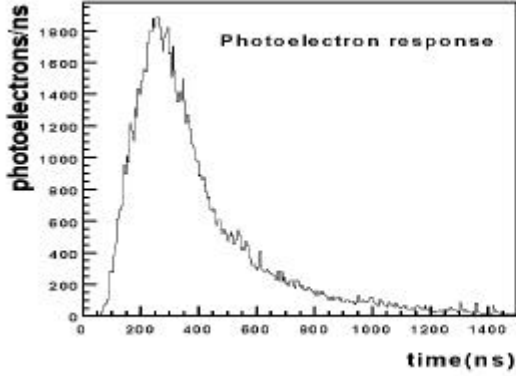


**Figure 4-a.** Time distribution of PEs in one PMT of a tank at 500 m from shower core for a vertical 1 ZeV proton shower.

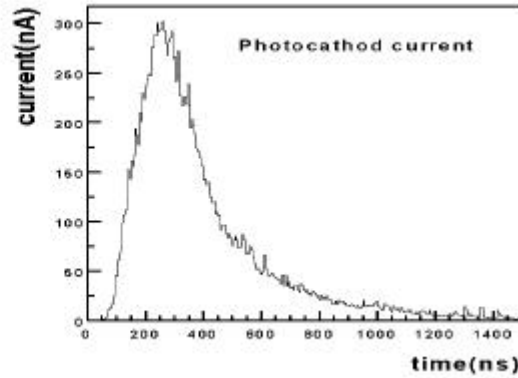


**Figure 4-b** Photocathode current for the same PMT

In order to quantify the effect of a  $2 \cdot 10^4$  PEs/25ns cutoff on typical showers, simulations were performed as explained previously for vertical and inclined protons at three different energies. The statistics were increased by randomly moving showers to different core positions with respect to the tank array. Tanks were considered only when the number of PEs detected by one of their PMTs was below the cutoff value and when the total number of PEs integrated over the signal duration time was above a threshold of 70 PEs corresponding to an equivalent of 2.5 vertical muons on a PMT. This threshold is a rough approximation of the local trigger.

Figure 5 shows distributions obtained for the number of tanks verifying the above conditions without cutoff and with the  $2 \cdot 10^4$  cutoff on the maximum number of PEs/25ns. In the case without the cutoff the mean number of tanks available for the reconstruction is about 21, 13 and 5 for vertical proton showers with incident energies of 1 ZeV, 100 EeV and 10 EeV, respectively. For the inclined showers at the same energies, the mean number of triggered tanks is larger with values of 27, 17 and 10 for the same energies. As can be seen, a cutoff of  $2 \cdot 10^4$  PEs/25ns would introduce only a very small decrease on the number of triggered tanks (about 1 tank). In all the considered cases the numbers of triggered tanks is above 4.

When comparing the case of a  $2 \cdot 10^4$  PEs/25ns cutoff with that of the  $10^5$  PEs/25ns cutoff, one can see that in most cases and for all type of showers no tanks are lost for the reconstruction. The probability of missing one tank by imposing the  $2 \cdot 10^4$  PEs/25ns cutoff is about 10%, 16% and 28% for respectively 10 EeV, 100 EeV and 1 ZeV vertical proton showers and it is 8%, 14% and 40% for inclined proton at the same energies. The probability of losing two tanks is less than 1%.

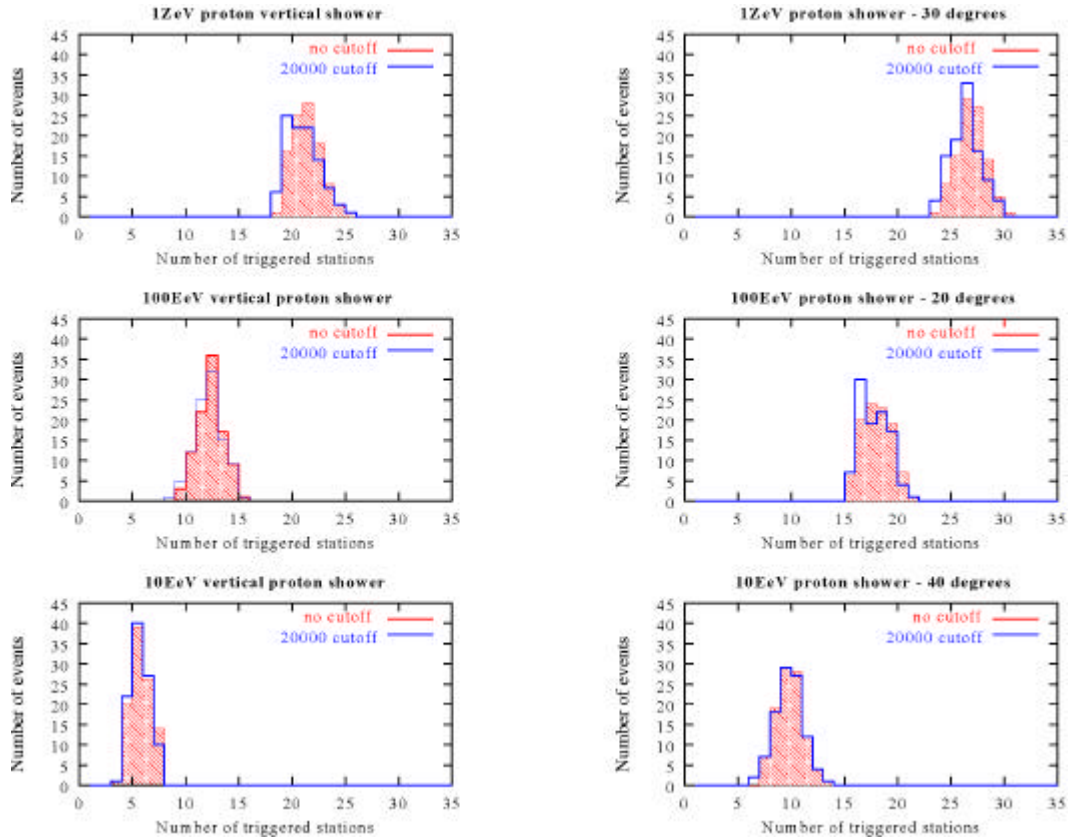


**Figure 5.** Histogram showing the number of tanks “triggered” for different showers at 1 ZeV, 100 EeV and 10 EeV. Each histogram is obtained with 100 different positions of the array respectively to the shower core.

Figure 6 shows the distance of the closest tank to the shower core for a 1 ZeV proton shower ( $r_{min}$ ). In the case without cutoff, this is always smaller than 1000 m, for obvious geometrical reasons. In the case of the  $2 \cdot 10^4$  PE/25ns cutoff, it varies from 550 m to about 1500 m.

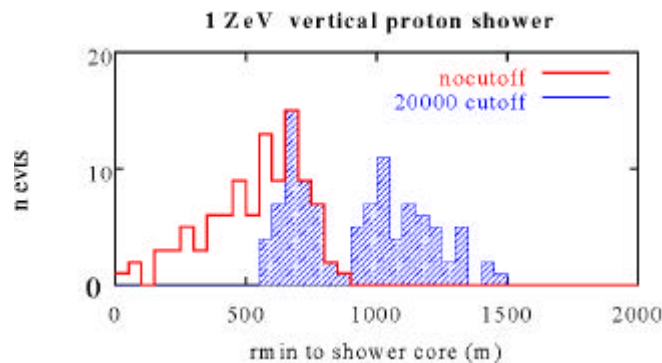


**Figure 6.** Distance of closest triggered tank for 100 1 ZeV vertical proton showers. The red curve corresponds to the case with no cutoff. The filled blue curve shows the case with the  $2 \cdot 10^4$  PE/25ns cutoff.

Table 2 shows the minimal and maximal distances of the closest measured tank from the shower core for the  $10^5$  PE/25 and  $2 \cdot 10^4$  PE/25ns cutoff. The photocathod current for a PMT in a tank at 500 m from core is also indicated.

Primary	Energy	Zenithal Angle	Peak current (nA)	Minimum value of rmin (m)	
				$10^5$ PEs/25ns cutoff	$2 \cdot 10^5$ PEs/ns cutoff
proton	500Eev	0	200	400	500
proton	500EeV	30	250	400	550
iron	500EeV	0	250	400	550
iron	500EeV	30	300	400	600
proton	1ZeV	0	300	400	550
proton	1ZeV	30	450	450	600

**Table 2.** Distances of closest tank to shower core from the simulation of 100 showers at each energy.

For the  $2 \cdot 10^4$  cutoff, the distance of closest tank (rmin) is pushed to 550–600 m for extreme energy showers, instead of 400-500m for a  $10^5$  cutoff. Due to the drastic decay of the density close to the shower core, a limitation of the upper range does not reduce dramatically the measurement zone around the shower core.

It is interesting to estimate the impact of the loss of this annular zone around the shower core on the probability to measure the shower within a given distance from the core. Figure 7 shows this detection probability as a function of the distance to the core for 10 different showers with different choices of cutoff. The green curves correspond to the ideal case where there is no cutoff at all. The yellow, light blue, pink, red and dark blue curves correspond to a cutoff of  $10^4$ ,  $2 \cdot 10^4$ ,  $3 \cdot 10^4$ ,  $5 \cdot 10^4$  and  $10^5$  PEs/25ns, respectively. For the low energy showers (10EeV) represented at the bottom of the figure, the impact of the different cutoff values is less than 10 %. At 100EeV, it is more of the order of 20 %. For extreme energy showers (above 500 EeV), the detection probability of the shower below 1000 m decreases by up to 30% for vertical showers when the cutoff is lowered from  $10^5$  PEs/25ns to  $2 \cdot 10^4$  PEs/25ns (the two blue curves). For inclined showers, the detection probability at the same distance decreases only by about 10%. Beyond 1100 m or so, all the cutoff values have the same effect. The  $2 \cdot 10^4$  PEs/25ns cutoff may result in a loss of accuracy in the energy measurement. However, the large number of triggered tanks for extreme showers should help to have a precise lateral profile beyond 1000m and compensate partly the lack of information.

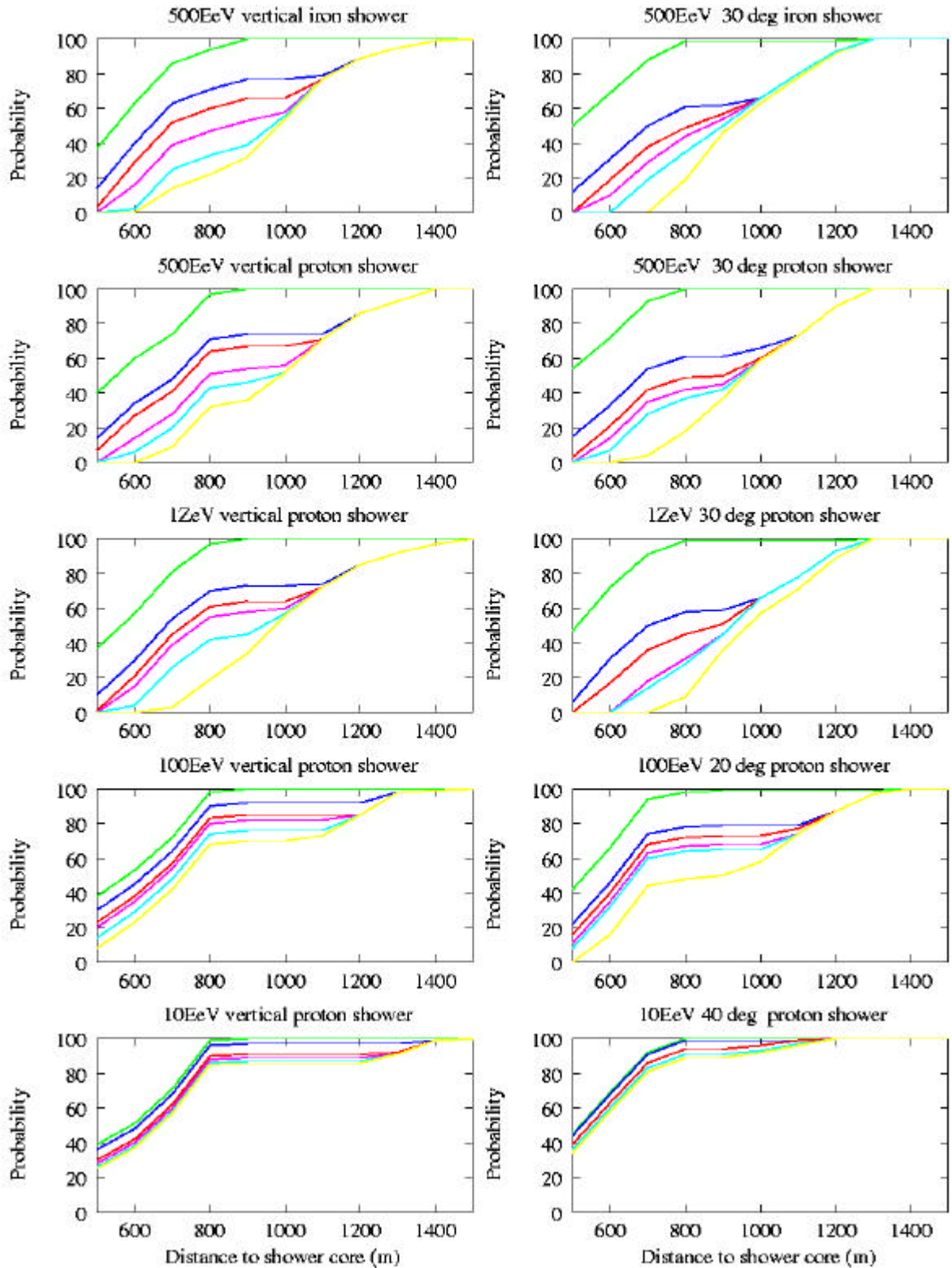


**Figure 7.** Detection probably under a distance to shower core as a function of the distance for 10 different showers. The six curves on each plot correspond to six different cases of cutoff (see in the text)

## Conclusions

In this note, we have studied the effect of the upper limit of the dynamic range on the shower detection. The calibration by background muons requires measurements at the level of a few photoelectrons. Moreover, the cross calibration between the anode and the dynode channels requires a sufficient overlap between the channels. In order to meet these requirements with the current electronics, a cutoff of the upper end of the dynamic range is necessary. We have shown that the lowest cutoff values ( $2 \cdot 10^4$  PE/25ns) in the proposed operation mode would only very slightly decrease the number of triggered tanks and would still allow to perform measurements at about 600 m from the shower core, even in the case of extreme energy showers.

## References:

- [1] The Pierre Auger Project, Design Report, November 1996.
- [2] J. Beatty, Preliminary design of the Auger Surface Electronics”, December 8, 1998 and private communication.
- [3] B. Genolini et al, GAP-2001-021.
- [4] T.Suomijärvi , GAP-2001-026.
- [5] M.A.Lawrence, R.J.O. Reid, and A.A. Watson, J. Phys. G17, 733 (1991).
- [6] A.M. Hillas, Proc 19<sup>th</sup> ICRC (La Jolla) 1,155 (1985).
- [7] S. J. Sciutto, AIRES, users guide and reference manual 2.2.0, GAP-99-020.
- [8] N.N. Kalmykov and S.S. Ostapchenko, Phys. At. Nucl., 56, (3) 346 (1993).
- [9] P. Billoir, GAP-2000-025 and private communication
- [10] C. Pryke, GAP-96-026.
- [11]10 T. Kutter et al., GAP-97-025.
- [12] L. Villaseñor et al., GAP-97-033.
- [13] P. Bauleo et al., NIM A 463 (2001) 175
- [14] The European Physical Journal C15 (2001) 151
- [15] H.Salazar et al , GAP-2001- 023
- [16] IPN-Orsay – INFN-Torino measurements, Malargue November 2000, private communication